Published in final edited form as:
Biochemistry. 2009 August 25; 48(33): 7794–7806. doi:10.1021/bi9004123.

RapA, SWI/SNF subunit of *Escherichia coli* RNA polymerase promotes the release of nascent RNA from transcription complexes

Brandon Yawn[1], **Lin Zhang**[1], **Cameron Mura**[2], and **Maxim V. Sukhodolets**[1,*]

[1]Department of Chemistry, Lamar University, Beaumont TX 77710

[2]Department of Chemistry, University of Virginia, Charlottesville VA 22904

Abstract

RapA, a prokaryotic member of the SWI/SNF protein superfamily, is an integral part of the RNA polymerase transcription complex. RapA's function and catalytic mechanism have been linked to nucleic acid remodeling. In this work we show that mutations in the interface between RapA's SWI/SNF and double-stranded nucleic acid-binding domains significantly alter ATP hydrolysis in purified RapA. The effects of individual mutations on ATP hydrolysis loosely correlated with RapA's nucleic acid-remodeling activity, indicating that the interaction between these domains may be important for the RapA-mediated remodeling of nonproductive transcription complexes. In this study we introduced a model system for *in vitro* transcription of a full-length *E. coli* gene (*slyD*). To study the function of RapA, we fractionated and identified *in vitro* transcription reaction intermediates in the presence or absence of RapA. These experiments demonstrated that RapA contributes to the formation of free RNA species during *in vitro* transcription. This work further refines our models for RapA function *in vivo* and establishes a new role in RNA management for a representative of the SWI/SNF protein superfamily.

Keywords

RapA; RNA polymerase; SWI/SNF; transcription; DNA-RNA; triplex

Escherichia coli (*E. coli*) has served as a primary model system for the study of enzymes involved in RNA synthesis. A textbook example of polymerase function, the *E. coli* core RNA polymerase formed by the $\alpha_2\beta\beta'\omega$ subunits is capable of transcription elongation and termination (1). Proteins called sigma factors (1–3) associate with the core enzyme and allow the resulting complex, referred to as the RNA polymerase holoenzyme, to bind DNA in a sequence-specific manner and initiate transcription from loosely homologous promoter sequences on the *E. coli* chromosome. Each sigma factor controls multiple groups of promoters; *e.g*, the key growth-related and housekeeping genes in *E. coli* are under control of σ^{70} (4), the *rpoD* gene product. Approximately one-third of the core *E. coli* RNA polymerase molecules in a given cell form a high-affinity, stoichiometric complex with σ^{70} under normal growth conditions; the $\alpha_2\beta\beta'\omega$ and $\alpha_2\beta\beta'\omega\sigma^{70}$ enzyme species display a number of distinct properties and can be chromatographically separated (5,6). Apart from the sigma factors and relatively small proteins (which are unlikely to display mechanistically complex enzymatic activities), the key known interactors of the *E. coli* RNA polymerase established through biochemical studies are NusA (7,8) and RapA (6,9). NusA – an essential RNA-binding protein in *E. coli* – has been described in the existing literature as a

*Correspondence: msoukhodol@my.lamar.edu, Phones: 409-880-7905 (office) 409-880-7906 (laboratory).

transcription elongation factor and a cofactor of antiterminators (10–13). The function of RapA (also known as HepA) – the first identified bacterial representative of the SWI/SNF protein superfamily – is not fully understood. Under most conditions (in liquid cultures), *rapA* deletion has little or no effect on cell growth (6,14), protein expression (as judged by 2D electrophoresis; M.V. Sukhodolets, unpublished results), UV-sensitivity (14), or mutation rates (14). This apparent lack of a pronounced *rapA* effect *in vivo* points to functions other than general regulation of transcription, as proposed for RapA's eukaryotic counterparts. However, *rapA* deletion results in a unique phenotype, rendering bacteria incapable of efficient growth on agar plates in high salt (15). *In vitro*, RapA promotes multi-round transcription in a salt concentration-specific fashion (15,16). Salt-selectivity is therefore a shared feature of RapA effects observed *in vivo* and *in vitro*. Our recent work presented multiple, independent lines of evidence indicating that RapA binds and remodels RNA during transcription (17). This study also indicated that non-canonical DNA-RNA complexes such as DNA-RNA triplexes – the formation of which is enhanced in high salt (17) – could represent potential substrates for RapA, and we proposed that remodeling of non-canonical nucleic acid complexes could be the primary function of RapA and its homologs *in vivo* (17). A recently reported, 3.2Å-resolution structure of RapA was used to construct a putative structural model for a RapA-nucleic acid complex, suggesting that RapA is capable of simultaneous interactions with both double-stranded and single-stranded nucleic acids (18). This is consistent with the proposed role of RapA in the remodeling of non-canonical nucleic acid complexes.

In this work we constructed several new RapA mutations, focusing on the RapA domain harboring SWI/SNF homology motifs IV–VI (referred to herein as the SWI/SNF domain) and its interface with the domain containing the putative double-stranded nucleic acid template (dsT)-binding site (17,18), and studied their effect on RapA's ATP-hydrolytic and nucleic acid-remodeling activities. We demonstrate a significant effect of the mutations in this region on RapA's ATP-hydrolytic and nucleic acid-remodeling activities. The effects of individual mutations on ATP hydrolysis loosely correlated with RapA's nucleic acid-remodeling activity in *in vitro* transcription, indicating that the interaction between the SWI/SNF and dsT-binding domains may be important for the RapA-mediated remodeling of nonproductive transcription complexes.

In this study we have tested – for the first time in studies with RapA – the effects of RapA on the transcription of a model full-length *E. coli* mRNA containing intact 5'-and 3'-nontranslated sequences. The results presented herein are in accord with our existing model, in which RapA aids RNA polymerase in the displacement of nascent RNA from transcription complexes. We show that this enzymatic activity of RapA is unique and cannot be mimicked by other RNA-binding proteins with a demonstrated ability to promote transcriptional cycling, such as S1 (19). In this work we further developed our methods for fractionation and identification of *in vitro* transcription reaction intermediates. Using a non-denaturing (as well as a previously developed semi-denaturing) method of separation of the *in vitro* transcription reaction intermediates, we demonstrate that RapA promotes the formation of non-DNA-bound or aggregated RNA species during transcription. This work further refines our models for RapA function *in vivo* and – taken together with our previous study – establishes a new role in RNA management for a representative of the SWI/SNF protein superfamily. This finding not only increases our understanding of the fundamental process of transcription, but also brings a fresh perspective to studies demonstrating links between mutations in human SWI/SNF genes and cancer (20–24).

Materials and Methods

Enzymes

In this study, we have further improved the procedure for the isolation of native *E. coli* RNA polymerase and its accessory proteins. The modified procedure – in general reminiscent to that described in (25) – results in improved purity of the isolated proteins and complexes. The key changes, in comparison with the protocol described in (25), included (a) the utilization of two different FPLC instruments: a classic (now discontinued) FPLC system (Pegasus Scientific), set up in the cold room to carry out the initial, single-stranded DNA chromatography stage, and an ACTA FPLC system (GE Healthcare) set up and operated at room temperature *via* Unicorn software during the final chromatography stages (however, the Superloops were placed on ice during the Mono Q column loading stage), (b) the utilization of self-prepared (calf thymus) single-stranded DNA-Sepharose 4B instead of commercially available DNA-Agarose, to improve flow rates, (c) scaling down the procedure to 25–35 g of *E. coli* MG1655 cells per purification and using a Mono Q 5/5 column in order to achieve more uniform loading of the column, and (d) increasing the length (>2-fold) of the Superdex 200 column during the final, gel-exclusion chromatography stage. The schematic for the procedure is shown in Figure S1B; the detailed protocol will be described elsewhere. Recombinant, *His*-tagged wild-type and mutant RapA proteins were purified as described in Figures S1C and S2. Wild-type recombinant S1 and NusA were isolated as previously described (25).

PCR and DNA purification

DNA encompassing the *slyD* operon was amplified from MG1655 *E. coli* chromosomal DNA using MS696 (5’-ATTGTAAGCTTCCCGGGGAAACGCCACCGCCACATTATTGAGGCG) and MS697 (5’-CCGAAAGTGGATCCCGGGGCCCGGCCTGTCAGGCGCAGGATTCAATGGCG)DNA primers and the Expand High Fidelity PCR kit (Roche Diagnostics). Reactions were carried out as suggested by the manufacturer; the extension time was 2 min at 72°C. Because our previous work implied the possibility of non-canonical interactions between nucleic acids in transcription, we tested different methods for purification of PCR-generated DNA templates in order to rule out potential impurity and/or conformational heterogeneity in the isolated DNA; the amplified DNA used in key experiments was purified by FPLC, as described in Figure S1, using a custom-packed 0.3-ml Source Q column. Following the DNA amplification, the reaction mixture was diluted 4–5-fold with purified water (KD Medical, Molecular Biology Grade) and injected onto the column. The reaction products were eluted with a linear gradient of NaCl (0–1 M) in 20 ml of TGED buffer (0.01 M Tris-HCl, 5% glycerol, 0.1 mM EDTA, 0.1 mM dithiothreitol, pH 7.5), as shown in Figure S1. The amplified *slyD* DNA – confirmed by agarose gel electrophoresis (Figure S1A, insert) and DNA sequencing during the primer extension experiments (Figure 4A) – was precipitated with 7–8 volumes of ethanol; air-dried pellets were then dissolved in purified water to the concentrations indicated below.

In vitro transcription

In vitro transcription reactions were carried out in either Buffer D (20 mM Tris-acetate, 10 mM magnesium acetate, 50 mM potassium acetate, 1 mM dithiothreitol, pH 7.9), Buffer C (50 mM Tris-HCl, 10 mM $MgCl_2$, 100 mM NaCl, 1 mM dithiothreitol, pH 7.9), or Buffer B (50 mM Tris-HCl, 10 mM $MgCl_2$, 200 mM NaCl, 1 mM dithiothreitol, pH 7.9); the transcription buffers are specified in Figure Legends. In our preliminary studies we found that the *slyD* mRNA was more efficiently synthesized *in vitro* in Buffer D than in the previously utilized Buffer B [17]). Since Buffer D is widely used as a standard buffer for a large number of bacterial restriction endonucleases and includes potassium and acetate (both

key ions in *E. coli*), we switched to Buffer D as a more 'physiological' buffer for *in vitro* transcription with linear DNA templates containing the *slyD* operon. Typically, 14-µl *in vitro* transcription reactions included 1.4 µl 10x reaction buffer, 2–4 µl purified linear DNA template containing the *slyD* operon (20–90 µg/ml in purified water) or 1–2 µl supercoiled DNA template pCPGt_3t_e (26) (0.3–0.4 µg/µl in purified water), 2 µl purified RNA polymerase holoenzyme (0.07–0.2 mg/ml in 1x TGED buffer, unless indicated otherwise in Figure Legends), 0.5–4 µl purified recombinant RapA (RapA concentrations are specified in Figure Legends), and purified water (KD Medical, Molecular Biology grade) to a volume of 12 µl. *In vitro* transcription was initiated by the addition of 2 µl of rNTP mix containing 1.4 mM each of ATP, GTP, CTP, UTP, and either [α-^{32}P] ATP or [α-^{32}P] UTP (MP Biomedicals). Reactions were incubated for 15 min at 37°C unless indicated otherwise. Transcription reactions were terminated by the addition of an equal volume (14 µl) of Stop solution (50% glycerol; 50 mM EDTA; Bromphenol Blue, 0.1%; pH 7.5), and 8-µl aliquots of the reactions were analyzed (without boiling, unless indicated otherwise) on either non-denaturing or semi-denaturing polyacrylamide gels. Semi-denaturing (0.4 mm-thick, 38 cm-long) gels were cast using the SequaGel kit (National Diagnostics); the exact polyacrylamide concentrations are specified in Figure Legends. Gibco BRL S2 sequencing gel apparatuses were used. Under semi-denaturing conditions (Figure 5), increasing gel thickness and reducing the sample volume led to a significant reduction in the yields of RapA-RNA and RNA polymerase-RapA-RNA complexes; we therefore believe that the complexes in question are not fully denatured by urea in the matrix of a 0.4 mm-thick gel during the course of these separations. Gels were typically run at 20–30 Watts until Bromphenol Blue reached the bottom of the gel, unless indicated otherwise. Non-denaturing (1 mm-thick, 32 cm-long) gels containing 1x TBE (KD Medical) were cast using ProtoGel polyacrylamide mix (National Diagnostics); Gibco BRL SA apparatuses were used. After electrophoresis, X-ray films (F-BX810; Phenix Research Products) were exposed to 'wet' gels covered with plastic wrap. With Kodak BioMax MS screens, typical exposure times were 8–40 hours at −80°C.

Primer extension experiments

20-µl primer extension reactions included 2 µl 10x M-MuLV Reverse Transcriptase Reaction Buffer, 6000–10000 cpm (^{32}P) end-labeled DNA primer MS702 (5'-CGCGCCAACAGCGACATCAAATTTGTCGCC), 2 µl dNTP mix (containing 1 mM each of dATP, dGTP, dCTP, and dTTP), 2 µl M-MuLV Reverse Transcriptase (New England Biolabs, 200,000 U/ml), 4 µl purified RNA from *in vitro* transcription reactions carried out as described above, and purified water to a final volume of 20 µl. Reactions were incubated for 30 min at 37°C and terminated and analyzed as described above for *in vitro* transcription reactions. Labeling and gel-purification of the DNA primer MS702 was performed as previously described for end-labeled RNA probes (17). Dideoxy DNA sequencing was carried out as described elsewhere.

Mutagenesis

The QuikChange™ site-directed mutagenesis kit (Stratagene) was used to construct the described RapA mutations. Primers LZ1 (5'-CAGCATCAGTGGCTGGTAGAAATGCTGGCCGCTTTCAACCTGCGCTTTGCGCTATTTGAT) and LZ2 (antiparallel to LZ1) were used to construct the RapA R221A/R222A double mutation. Primers BY3 (5'-GAGCAGCGTATTGGTCGTCTGGATGCTATCGGCGCGGCGCACGATATTCAGATCCATGTG) and BY4 (antiparallel to BY3) were used to construct the RapA R599A/Q602A mutation, and primers BY5 (5'-GCTATTAAAGTCTCCGGCATTATGGGCGCAGCTGCAAGTGCGGAAGATCGTGCTCGCGATATGCTC) and BY6 (antiparallel to BY5) were used to construct the RapA

R457A/K458A mutation. Following amplification with mutagenic primers and *Dpn*I digestion of the template DNA (pQE32-RapA [17]), aliquots of the reaction mixtures were used to transform XL10-Gold Ultracompetent Cells (Stratagene). Plasmid DNAs from individual clones were purified and analyzed. The constructs were confirmed by DNA sequencing. The expression of full-length RapA in individual clones was also verified by SDS-PAGE-Western Blot using RapA-specific antibodies (14). The purified plasmids carrying the constructed mutation(s) were then re-transformed into M15/pRep4 *E. coli* competent cells (Qiagen), and the *His*-tagged RapA protein was overproduced and purified as described above.

Western blotting was carried out as follows. Following electrophoresis, proteins were transferred onto either Immobilon-P (Millipore) or Hybond-P (Amersham Pharmacia Biotech) membranes (with similar results) in Mini-PROTEAN 3 Trans-Blot modules (Bio-Rad), typically, at 40–60 V overnight. Membranes were blocked with 5% Blotting Grade Blocker (Bio-Rad; #170–6404) in PBST (Calbiochem; #524653) for 30–60 min and incubated with primary antibodies (typically, a rabbit serum at a dilution of 1/1000 to 1/5000 in 1x PBST containing 1% Blotting Grade Blocker) for 1–5 hours at room temperature on an orbital shaker. Following three 5-min washes with 1x PBST, membranes were incubated with secondary antibodies (a donkey anti-rabbit Ig–horseradish peroxidase conjugate [Amersham Pharmacia Biotech], typically at a dilution of 1/2000 to 1/16000 in 1x PBST containing 1% Blotting Grade Blocker) for 30–60 min. Following three 5-min washes with 1x PBST, and 2–3 brief washes with water, the membranes were incubated for 30 sec with 2–4 ml of SuperSignal West Pico Chemiluminescent Substrate (Pierce; #34080), briefly drained, and placed in plastic wrap; X-ray films (Phenix Research Products; F-BX810) were then exposed to the luminescent membranes.

ATPase activity assays

ATPase activity assays were performed by measuring the amount of [α-^{32}P]ADP released from [α-^{32}P]ATP. Either Buffer D or Buffer C was used as a reaction buffer, with similar results; reaction buffers are specified in Figure Legends. Ten-μl reaction mixtures contained 1 μl of the 10x reaction buffer, 0.3–0.5 μg purified RapA, 50–1600 nM cold ATP, and 500–3000 cpm of [α-^{32}P]ATP (MP Biomedicals; #32007U). Following incubation at 37°C (typically for 60 min, unless indicated otherwise in Figure Legends), 1.5–3 μl from each reaction was spotted on a PEI-cellulose plate (Analtech; #206016), and chromatography was carried out in 1 M LiCl, 1 M formic acid. Following chromatography, the plates were covered with plastic wrap, and X-ray films (Phenix Research Products; F-BX810) were exposed to the TLC plates.

E. coli strains

The previously constructed MG1655*rapA*$^{-}$ *E. coli* strain (14) was used in this work.

Results

Functional significance of RapA for bacterial growth

Although the *rapA* gene is not essential in *E. coli* (14), *rapA* deletion results in a unique phenotype manifested as the inability of *E. coli* to grow efficiently on LB agar containing 1M NaCl (15). We recently explained this phenotype in light of our newly rendered model for RapA function in the remodeling of noncanonical DNA-RNA complexes in transcription (17), the formation of which is enhanced in high salt (17). To study this phenotype further, we (a) analyzed the kinetics of growth of *E. coli* MG1655*rapA*$^{+}$ and MG1655*rapA*$^{-}$ strains on LB-agar plates in the presence of NaCl and other salts, and (b) compared growth efficiencies of the two strains on agar plates with those in liquid media. Kinetic experiments

indicated a pronounced effect of *rapA* on cell growth at ≥0.5 M NaCl. Prolonged incubations of the plates (20–40 hours) containing 0.5–0.75 M NaCl resulted in significant differences in colony size between the two strains (Figure 1A). The effects were more pronounced on LB-agar plates than on SOC-agar or Superbroth-agar plates (data not shown). The effect of salts other than NaCl on growth of the two strains in plated cultures is illustrated in Figure 1B. Interestingly, the growth defect associated with the *rapA* deletion mutation was not evident in the liquid media – under otherwise similar conditions – but was seen only in plated cultures. As an alternative means of increasing the intracellular ionic strength in liquid cultures, we monitored the kinetics of growth of the *rapA*$^{+}$ and *rapA*$^{-}$strains in the presence of polyethylene glycol. However, these experiments consistently showed little or no difference in growth rates between the two strains, even at relatively high polyethylene glycol concentrations (data not shown).

Alterations of ATP-hydrolytic and nucleic acid-remodeling activities of RapA by mutations in the interface between RapA's SWI/SNF and dsT-binding domains

We sought to extend previously developed *in vitro* assays for analysis of the function of individual domains in RapA. Our primary focus was the RapA domain harboring SWI/SNF homology motifs IV–VI (referred to herein as the SWI/SNF domain), due to its obvious significance in defining the SWI/SNF protein superfamily. Studies with distant homologs of RapA have indicated that coordinated, ATP-driven re-orientation of the SWI/SNF domain with respect to the double-stranded nucleic acid-binding domain may enable translocation of SNF2 enzymes along nucleic acids (27,28). We therefore sought to genetically alter the interface of the two domains in RapA (Figures 2A and 2B) in order to determine the effect of such modifications on RapA's ATP-hydrolytic and nucleic acid-remodeling activities. To this aim, we constructed and purified two mutant RapA proteins (each carrying a double mutation): RapA$^{R599A/Q602A}$ (this conserved amino acid pair is located within the section of RapA's SWI/SNF domain facing the dsT-binding domain [Figures 2A and 2B]), and RapA$^{R221A/R222A}$ (this moderately conserved arginine tandem is positioned in the section of RapA's dsT-binding domain facing the SWI/SNF domain [Figures 2A and 2B]). Each double mutation – based on available structural data (18) – should result in destabilization of the interaction between RapA's dsT-binding and SWI/SNF domains. The purification of both mutant proteins is described in Supplementary Data (Figures S2A and S2B). The second set of mutations targeted a potential single-stranded nucleic acid-binding site within RapA's SWI/SNF domain. Recent work indicated that RapA's SWI/SNF domain could be involved in binding single-stranded nucleic acids (18). The model of the RapA-nucleic acid complex introduced by Shaw et al. suggests that the loop within RapA's SWI/SNF domain carrying a conserved tandem of positively charged amino acids (R457/K458 [Figures 2A and 2B]) may be involved in this interaction (18). We therefore constructed and purified a RapA mutant carrying alanine substitutions at these two amino acid positions (RapA$^{R457A/K458A}$; Supplementary Data, Figure S2C).

Mutations in the interface of RapA's dsT-binding and SWI/SNF domains altered ATP hydrolysis by purified RapA, as expected. The RapA R599A/Q602A mutation abolished ATPase activity in purified mutant RapA (Figures 2C and 2D; the solubility and yields of RapA$^{R599A/Q602A}$ were comparable to those seen with wild-type RapA [Figures S2B and S2D]). In contrast, the RapA R221A/R222A mutation resulted in an increase in ATPase activity in the purified protein (Figures 2C and 2D); the effect was primarily due to an increase in k_{cat} (Figure 2D). Because this is the first case to date in which a RapA mutation resulted in an increase in RapA's specific ATPase activity, we carried out multiple, side-by-side purifications of wild-type RapA and RapA$^{R221A/R222A}$; during the course of these trials we consistently observed higher specific ATPase activities with purified RapA$^{R221A/R222A}$ (a representative side-by-side comparison of specific ATPase activities in proteins obtained

in an independent set of purification procedures is shown in [Supplementary Data Figure S3]). The RapA R457A/K458A double mutation had little or no effect on ATP binding ($K_{m,\ ATP}$) and hydrolysis (Figure 2D). This result is expected and is consistent with the predicted position of these amino acids in the section of RapA's SWI/SNF domain opposite from the putative ATP-binding site (18).

Next, we monitored ATP hydrolysis by wild-type and mutant RapA proteins in the presence or absence of ssRNA, a (ds)RNA-DNA hybrid, and dsDNA. There was no apparent effect of these nucleic acids on the rates of RapA-mediated ATP hydrolysis (Supplementary Data, Figure S4). This result is in accord with previously reported data indicating little or no modulation of RapA's ATPase activity by nucleic acids (6) (in contrast to the Rad54 homolog from *Sulfolobus solfataricus* [*Sso*Rad54], the ATPase activity of which is stimulated by nucleic acids [29]). Because it was reported that RNA polymerase exerts a stimulatory effect on k_{cat} of the RapA ATPase (6) we also monitored the ATP hydrolysis by wild type and mutant RapA proteins in the presence or absence of RNA polymerase. We found that $RapA^{R221A/R222A}$ (the specific ATPase activity of which was comparable to that of wild-type RapA in the presence of the polymerase) was insensitive to the stimulatory effect of the polymerase (Figure 2E, compare lanes 3 and 4 to lanes 5 and 6). ATP hydrolysis was detectable in reactions containing $RapA^{R599A/Q602A}$ in the presence of the polymerase – an apparent partial recovery of the ATP-hydrolytic function in the $RapA^{R599A/Q602A}$-core enzyme complex (Figure 2E, compare lanes 3 and 4 to lanes 7 and 8). The $RapA^{R457A/K458A}$ double mutant mimicked the behavior of wild-type RapA (Figure 2E, compare lanes 3 and 4 to lanes 9 and 10).

Next, we compared the transcription-stimulatory activities of the constructed RapA mutants with that of wild-type RapA. In this set of experiments we used an extensively characterized supercoiled DNA template (pCPGt_3t_e) containing the *T7A1* promoter (26; also see refs. 15–17). In the case of $RapA^{R221A/R222A}$ and $RapA^{R599A/Q602A}$, the effects of the mutations on the transcription-stimulatory activity correlated with those on ATP-hydrolytic activity (*i.e.*, there was little or no transcription-stimulatory effect in the presence of excess $RapA^{R599A/Q602A}$ and there was a transcription-stimulatory effect comparable to or exceeding that of wild-type RapA in the case of $RapA^{R221A/R222A}$)(Figure 3). $RapA^{R457A/K458A}$ was largely ineffective in promoting transcriptional cycling under these conditions (Figure 3, compare lanes 2 and 5), even though its ATP-hydrolytic activity was comparable to that of wild-type RapA (Figures 2C and 2D).

Selection and characterization of a model system for *in vitro* transcription of a complete *E. coli* gene

To date, the effects of RapA on the synthesis of relatively long and less structured (*i.e.* more physiologically relevant) RNAs have not been thoroughly studied. This apparent shortcoming of our previously used model systems prompted us, in the present work, to focus on the effects of RapA on the transcription of a complete *E. coli* model gene possessing intact 5' and 3' nontranslated sequences. Although a number of model systems for *in vitro* transcription of *E. coli* genes have been described, they did not fully meet our selection criteria, which included requirements for (a) a robust promoter resulting in a relatively high copy number of the translated protein product, (b) a transcribed gene constituting an independent transcription-translation unit (to avoid polar effects in genetic studies), (c) the exhibition of a relatively benign enzymatic activity by the translated protein, and (d) a size of ≤1kb (to facilitate the analysis of DNA-bound transcription complexes on polyacrylamide gels). After some preliminary work, we selected the *E. coli slyD* gene, which encodes a 21.2-kDa protein bearing the same name (referring to the observation that mutations in the *slyD* gene result in sensitivity to lysis by bacteriophage [30]). SlyD is an abundant protein chaperone with demonstrated peptidyl-prolyl cis-trans isomerase

(rotamase) activity (31–33) and is a frequent contaminant during the metal affinity resin purification of His-tagged proteins (34–36). Indeed, we identified SlyD by mass spectrometry during the purification of recombinant RapA (Supplementary Data, Figure S1C, bottom panel). During the course of our preliminary work, we (a) amplified and purified DNA containing the *slyD* gene and its promoter and confirmed its ability to support a promoter-specific RNA polymerase transcriptional activity (see below, Figure 5 and Figure 6), and (b) mapped the *slyD* promoter(s) and determined the exact transcription sites for the RNA polymerase holoenzyme by the primer extension method (Figure 4). Primer extension indicated two distinct transcription start sites – both, conventionally, A's (Figure 4A; the nontranslated 5'-termini of the *slyD* mRNAs are shown in Figure 4D). The tandem *slyD* promoters (denoted P1 and P2) share homology with known *E. coli* promoters (Figure 4B). Primer extension experiments indicated little or no non-promoter-specific initiation during *in vitro* transcription (Supplementary Data, Figure S5). We also (c) determined the approximate position of the *slyD* gene's transcription terminator (loosely mapped to the tandem hairpins located immediately downstream from the *slyD* gene) (Supplementary Data, Figure S6); the efficiency of termination *in vitro* at this intrinsic *slyD* terminator was consistently high (>80%; Supplementary Data, Figure S6). Taken together, these results are in accord with the existing *E. coli* databases, which indicate that the *slyD* gene is transcribed and translated independently. In summary, the PCR-generated DNA templates encompassing the *slyD* operon met most of our criteria, so we proceeded to the experiments addressing the effects of RapA.

Effect of RapA on transcription of the *slyD* gene *in vitro* and identification of the reaction intermediates

Semi-denaturing fractionation of *in vitro* transcription intermediates—In our previous work, semi-denaturing fractionation of *in vitro* transcription complexes was instrumental for the detection of RapA-transcript and RNA polymerase-RapA-transcript intermediates (17). We now used a similar approach to test what effect (if any) the addition of purified RapA would have on synthesis of the *slyD* mRNA. In the absence of RapA, RNA polymerase produced little or no detectable non-protein-bound or aggregated transcripts in the samples not denatured by boiling (Figure 5A, lanes 1 and 3). In contrast, reaction mixtures containing RapA consistently yielded non-DNA-bound or aggregated RNA (Figure 5). Next, we tested whether S1 – the RNA-binding ribosomal protein capable of stimulating transcriptional cycling (likely, *via* cooperative interaction with nascent RNA in a co-transcriptional manner [19]) – could mimic the observed activity of RapA. These experiments showed that excess S1 failed to promote an RNA release similar to that seen with RapA (resulting in the transcript's appearance as non-DNA-bound or aggregated species in gel-fractionated reactions)(Figure 5A, compare lanes 2 and 3). On low-percent (<5%) polyacrylamide gels we were able to discriminate clearly between DNA-bound and non-DNA-bound transcripts through selective ^{32}P RNA or DNA labeling (Figure 5B). The kinetics experiments demonstrated the RNA displacement at early (5-min) time-points (Figure 5C, lanes 7 and 8). An increase in the RNA polymerase/DNA template molar ratio, while boosting the overall yield of the transcript, promoted the formation of large complexes incorporating nascent RNA. Nevertheless, the activity of RapA was also apparent at late time points under these conditions (Figure 5C, lanes 3–6). Titration of the *in vitro* transcription reactions with purified RapA and identification of the RapA-specific reaction intermediates is shown in Figure 5D.

Non-denaturing fractionation of *in vitro* transcription intermediates—To rule out the possibility that the presence of urea accounted for the observed RNA displacement, we carried out PAGE-based fractionations of the *in vitro* transcription mixtures under non-denaturing conditions (in the absence of urea)(Figure 6A). The ability of RapA to

displace ^{32}P-labeled RNA from transcription complexes or aggregates was apparent on non-denaturing gels (Figure 6A); however, a loss of definition in the separation of individual complexes was apparent under non-denaturing conditions.

Next, we compared wild type RapA with mutant RapA proteins side-by-side in *in vitro* transcription reactions with DNA templates containing the *slyD* operon (Figure 6B). In general, the effects of wild-type and mutant RapA proteins on the levels of free (non-DNA-bound or aggregated) *slyD* mRNA observed under these conditions were comparable to those seen in *in vitro* transcription studies with supercoiled DNA template containing the *T7A1* promoter (in which the reaction products were fractionated in the presence of urea [Figure 3]).

We carried out non-denaturing (G-25 Sephadex cartridge-based) purifications of non-productive transcription complexes containing ^{32}P-labeled RNA transcript (Figure 6C, right panels) and tested their stability in the presence or absence of RapA and ATP. These experiments indicated an ATP-dependent reduction in the levels of DNA-bound or aggregated RNA in the presence of RapA (Figure 6C, graph).

Discussion

RapA, a prokaryotic representative of the SWI/SNF superfamily, was identifed through biochemical studies as a subunit of the *E. coli* RNA polymerase complex (6,14). *In vitro*, excess RapA promotes multi-round transcription (15,16). To investigate RapA's nucleic acid substrate specificity and the mechanism of its transcription-stimulatory activity, our group analyzed nucleic acid-binding and remodeling activities of RNA polymerase-RapA complexes (17). In this work we sought (i) further advances in genetic analyses of RapA (specifically, to extend genetic approaches to understanding the explicit functions of individual RapA domains), (ii) further development of biochemical methods for trapping functionally significant transcriptional intermediates, and (iii) to introduce a model system for *in vitro* transcription of a complete *E. coli* gene for future biochemical and genetic studies.

Functional significance of RapA

To obtain additional insights into *rapA* function *in vivo*, we have further studied the *E. coli* (MG1655) *rapA* deletion strain. Importantly, we demonstrate that the pronounced slow-growth phenotype resulting from the *rapA* deletion mutation are seen only in plated (but not in liquid) cultures. We speculate that this may be due to the *E. coli* cell's increased ability to utilize its ionic pumps in liquid media in order to lower the intracellular salt concentration (thus reducing the potentially negative impact of salt-induced interactions between nucleic acids). To date, this is the first study demonstrating that the distinct slow-growth phenotype associated with the *rapA* deletion mutation can be observed at physiological osmolarity (Figure 1B). Based on this evidence, we argue that the perception of *rapA* as a gene that contributes only marginally to *E. coli* physiology may not be fully correct.

RapA mutagenesis

RapA mutations described in this work targeted the interface of RapA's putative double-stranded nucleic template (dsT)-binding and SWI/SNF domains and the cluster of positively charged amino acids within RapA's SWI/SNF domain (R457/K458) – a tentative single-stranded nucleic acid-binding site (and a possible binding site for an RNA strand invading duplex DNA in our model for RapA function [17]) (Figure 2B; ssT). Mutations at the interface of RapA's dsT-binding and SWI/SNF domains altered RapA's ATPase activity (Figures 2C and 2D). These results are consistent with the predicted position of RapA's

ATP-binding site at the interface of the two aforementioned domains (18). The constructed mutations also altered the transcription-stimulatory activity of RapA and its ability to displace RNA from transcription complexes. In general, the effects of individual mutations on ATP hydrolysis correlated with RapA's transcription-stimulatory activity, indicating that the interaction between the SWI/SNF and dsT-binding domains may be important for RapA-mediated remodeling of nonproductive transcription complexes. The significant negative effect of the R599A/Q602A double mutation (in the recently reported RapA structure [18], these two amino acids are in close proximity) on ATP hydrolysis and the concomitant loss of the protein's transcription-stimulatory activity may be due to a general relaxation of the structure of the SWI/SNF domain (as a result of the loss of an internal stabilizing link) and its expansion into the ATP-binding cleft. Remarkably, the interaction with RNA polymerase enabled partial restoration of RapA$^{R599A/Q602A}$'s ATP-hydrolytic function; this result may point to the possibility of re-orientation of RapA's SWI/SNF domain with respect to the (putative) double-stranded nucleic acid-binding domain, as proposed for the *Sso*Rad54 protein (27). The effect of the R221A/R222A mutation – which generated a protein with transcription-stimulatory activity exceeding that of wild-type RapA (albeit, insensitive to RNA polymerase regulation) – also seems to support the notion that the stimulation of RapA's ATP-hydrolytic activity by RNA polymerase may involve re-orientation of RapA's SWI/SNF domain with respect to the double-stranded nucleic acid-binding domain.

Effects of RapA on *in vitro* transcription of the *slyD* mRNA

In this work, we developed an *in vitro* transcription system of a complete model *E. coli* gene (*slyD*). We monitored the *in vitro* synthesis of *slyD* mRNA and fractionated *in vitro* transcription reaction intermediates (identified through a combination of selective ^{32}P-labeling and immunoassays) by PAGE. Our data unambiguously demonstrate that RapA promotes the formation of non-DNA-bound or aggregated RNA species during *in vitro* transcription (Figure 5 and Figure 6). This result is in accord with the results of our previous study utilizing supercoiled DNA templates and an all-native-enzymes system (17). Under most conditions, RapA promoted the formation of (non-DNA-bound) RNA polymerase-transcript complexes. Previously reported RapA-transcript complexes were also detected during the course of this study (e. g. see Figures 5C and 5D). It seems unlikely that the formation of non-DNA-bound or aggregated RNA species in the presence of RapA was due to a general increase in the yield of RNA. (i) Generally, in this set of experiments (Figure 5 and Figure 6) we avoided extended incubations of the *in vitro* transcription mixtures in order to minimize potential contributions of RapA to transcriptional cycling. (ii) RapA promoted the formation of non-DNA-bound or aggregated transcript (effectively redistributing RNA in the system) under conditions in which there was clearly no increase in the transcript yield in the presence of RapA (for example, see Figure 5C, lanes 3–6). (iii) The experiments with the purified non-productive transcription complexes (Figure 6C) also indicate that RapA contributes to transcript release. Under most experimental conditions, little or no free (non-RNA polymerase-bound or aggregated) *slyD* mRNA was generated during *in vitro* transcription in the absence of RapA, perhaps pointing to mechanistic limitations in the *in vitro* synthesis of longer, less structured RNAs.

The function(s) of RapA

The homology of RapA to SWI/SNF proteins and more distant DEAD/H family helicases (37,38) points to roles in nucleic acid remodeling. RapA's status as an accessory RNA polymerase subunit (6,14,15,17) indicates that this nucleic acid-remodeling activity is likely linked to transcription. In accord with this, RapA promotes the disruption of noncanonical DNA-RNA complexes (putative DNA-RNA triplexes) in an ATP-dependent manner (17). RNA is a likely substrate of RapA, based on multiple, independent lines of evidence summarized in our recent work (17). In that study, we proposed that RapA could track DNA

along with the RNA polymerase core enzyme in order to disrupt non-canonical DNA-RNA complexes (17). The salt-selectivity of RapA's *in vivo* and *in vitro* activities supports this model for RapA function.

The results presented herein indicate that RapA contributes to the formation of free (non-DNA-bound or aggregated) RNA species during transcription. RNA polymerase without RapA failed to efficiently generate *slyD* mRNA from linear DNA templates containing the *E. coli slyD* operon. Our recent studies suggested that nonproductive interactions by nascent RNA could represent a key obstacle to continuous transcriptional cycling (19; also see 17). In the latter work we proposed that noncanonical complexes between dsDNA and transcript RNA (such as dsDNA-RNA triplexes) could form during transcription and impede the activity of 'trailing' RNA polymerase molecules. The formation of putative dsDNA-ssRNA triplexes is supported by a classic work by Roberts and Crothers (39), as well as several recent studies (17,40,41). RapA-mediated displacement of relatively long transcripts from DNA (as observed in this study under non-denaturing conditions [Figure 6]) argues that RapA may possess an independent nucleic acid-remodeling activity. The possibility that relatively long transcripts could be wrapped around DNA (in a less orderly fashion than that found in a conventional Hoogsteen triplex) as a result of the polymerase's tracking of a helical, linear DNA molecule has been previously considered (42). RapA could disrupt these noncanonical DNA-RNA complexes by either riding with the polymerase while trawling the RNA (Figure 7A, *Model A1* [the 'minesweeper' model]) or acting as a dsDNA-ssRNA topoisomerase (*Model A2*; schematic is not shown). Well-documented, nonproductive ternary complexes in which nascent RNA's 3'-end is extruded (43–45) also could represent potential substrates for RapA. RapA could contribute to RNA release by either extracting the misaligned RNA or transporting the polymerase along DNA (thus acting as a translocase), both scenarios resulting in re-alignment of the core enzyme's active site with the 3'-end of the RNA (Figure 7B, *Model A3*) and subsequent RNA release. Finally, the possibility of RapA disrupting complexes formed between transcripts synthesized on different DNA molecules ('*in trans*')(*Models B*; schematic is not shown) also cannot be entirely ruled out.

Both the current study and our preceding work point to RNA as a substrate of RapA. It is therefore interesting to question whether the RNA-directed activities of RapA may overlap to some extent with those of Rho – an extensively studied RNA-binding protein with established roles in transcription termination (for review and a complete set of references see [46]) – particularly, in light of Rho's known ATP-dependent helicase activity with respect to DNA-RNA hybrids and its demonstrated ability to enhance RNA release from transcription elongation complexes. Testing RapA and Rho side-by-side may shed new light on the functions of these two proteins and is likely to be a part of our future studies of *E. coli* transcription.

In summary, in this work we (a) reported *in vivo* data demonstrating functional significance of the *rapA* gene under physiological osmolarity, (b) introduced and characterized a model system for the *in vitro* synthesis of *E. coli slyD* mRNA and further developed techniques for non-denaturing fractionation of transcription intermediates, and (c) described several new mutations in RapA's SWI/SNF domain and its interface with the (putative) double-stranded nucleic acid template-binding domain. The RapA R221A/R222A and R599A/Q602A mutations described in this study (both of which resulted in alterations in RapA's ATPase activity with no apparent effect on protein folding or solubility) represent a valuable asset for future studies. Both mutant proteins, along with the ribosomal protein S1, could serve as controls for ATP-dependent and ATP-independent RapA activities. Finally, (d) in this work we further refined our models for RapA function *in vivo*. Our future studies will address the mechanistic aspects of RapA's enzymatic activity in terms of its compatibility with one or

more of the models proposed herein. We will also carry out genetic studies designed to identify potential *rapA* interactors in *E. coli*.

Supplementary Material

Refer to Web version on PubMed Central for supplementary material.

Acknowledgments

We thank Timothy Gallaher at the University of Southern California School of Pharmacy for the mass spectrometry analyses of RapA and SlyD, Karen Sukhodolets, and anonymous reviewers for helpful comments and suggestions. This work was supported in part by Grant Number R15GM081803 from the National Institute of General Medical Sciences (to M.V.S.) (the content of this study is solely the responsibility of the authors and does not necessarily represent the official views of the National Institute of General Medical Sciences or the National Institutes of Health), a Welch Foundation grant (V-0004), and departmental funds.

Funding: this work was supported in part by Grant Number R15GM081803 from the National Institute of General Medical Sciences (to M.V.S.), a Welch Foundation grant (V-0004), and departmental funds

Abbreviations

ATP	adenosine-5’-triphosphate
CTP	cytidine-5’-triphosphate
ds	double-stranded
FPLC	fast protein liquid chromatography
GTP	guanosine-5’-triphosphate
RNAP	RNA polymerase
PAGE	polyacrylamide gel electrophoresis
PEI	polyethylenimine
PBS	phosphate buffered saline
PBST	PBS-Tween
RNAP	RNA polymerase
ss	single-stranded
TBE	Tris-borate-EDTA
TLC	thin layer chromatography
UTP	uridine-5’-triphosphate

References

1. Burgess, RR.; Erickson, B.; Gentry, D.; Gribskov, MM.; Hager, D.; Lesley, S.; Strickland, M.; Thompson, N. RNA polymerase and the Regulation of Transcription. New York: Elsevier Science Publishing Co., Inc.; 1987. p. 3-15.
2. Gross, CA.; Lonetto, M.; Losick, R. Transcriptional Regulation. Yamamoto, K.; McKnight, C., editors. Cold Spring Harbor, NY: Cold Spring Harbor Laboratory Press; 1992. p. 129-176.
3. Maeda H, Fujita N, Ishihama A. Competition among seven *Escherichia coli* σ subunits: relative binding affinities to the core RNA polymerase. Nucleic Acids Res. 2000; 28:3497–3503. [PubMed: 10982868]
4. Burgess RR, Travers AA, Dunn JJ, Bautz EK. Factor stimulating transcription by RNA polymerase. Nature. 1969; 221:43–46. [PubMed: 4882047]

5. Hager DA, Jin DJ, Burgess RR. Use of Mono Q high-resolution ion-exchange chromatography to obtain highly pure and active *Escherichia coli* RNA polymerase. Biochemistry. 1990; 29:7890–7894. [PubMed: 2261443]
6. Sukhodolets MV, Jin D. RapA, a novel RNA polymerase-associated protein, is a bacterial homolog of SWI2/SNF2. J. Biol. Chem. 1998; 273:7018–7023. [PubMed: 9507009]
7. Greenblatt J, Li J. Interaction of the sigma factor and the *nusA* gene protein of *E. coli* with RNA polymerase in the initiation-termination cycle of transcription. Cell. 1981; 24:421–428. [PubMed: 6263495]
8. Friedman, DI.; Gottesman, M. Lambda II. Cold Spring Harbor, NY: Cold Spring Harbor Laboratory Press; 1983. p. 21-51.
9. Muzzin O, Campbell EA, Xia L, Severinova E, Darst SA, Severinov K. Disruption of *Escherichia coli* hepA, an RNA polymerase-associated protein, causes UV-sensitivity. J. Biol. Chem. 1998; 273:15157–15161. [PubMed: 9614128]
10. Horwitz RJ, Li J, Greenblatt J. An elongation control particle containing the N gene transcriptional antitermination protein of bacteriophage lambda. Cell. 1987; 51:631–641. [PubMed: 2445491]
11. Squires CL, Greenblatt J, Li J, Condon C, Squires CL. Ribosomal RNA antitermination *in vitro*: requirement for Nus factors and one or more unidentified cellular components. Proc. Natl. Acad. Sci. USA. 1993; 90:970–974. [PubMed: 8430111]
12. Das A, Pal M, Mena JG, Whalen W, Wolska K, Crossley R, Rees W, von Hippel PH, Costantino N, Court D, et al. Components of multiprotein-RNA complex that controls transcription elongation in *Escherichia coli* phage lambda. Methods in Enzymology. 1996; 274:374–402. [PubMed: 8902820]
13. Gusarov I, Nudler E. Control of intrinsic transcription termination by N and NusA: the basic mechanisms. Cell. 2001; 107:437–449. [PubMed: 11719185]
14. Sukhodolets M, Jin D. Interaction between RNA polymerase and RapA, a bacterial homolog of SWI2/SNF2. J. Biol. Chem. 2000; 275:22090–22097. [PubMed: 10801781]
15. Sukhodolets MV, Cabrera JE, Zhi H, Jin DJ. RapA, a bacterial homolog of SWI2/SNF2, stimulates RNA polymerase recycling in transcription. Genes Dev. 2001; 15:3300–3341.
16. Sukhodolets MV, Garges S, Jin DJ. Purification and activity assays of RapA, the RNA polymerase-associated homolog of the SWI/SNF superfamily. Methods Enzymol. 2003; 370:283–290. [PubMed: 14712653]
17. McKinley BA, Sukhodolets MV. *Escherichia coli* RNA polymerase-associated SWI/SNF protein RapA: evidence for RNA-directed binding and remodeling activity. Nucleic Acids Res. 2007; 35:7044–7060. [PubMed: 17913745]
18. Shaw G, Gan, Jianhua, Zhou Y, Zhi H, Subburaman P, Zhang R, Joachimiak A, Jin D, Ji X. Structure of RapA, a SWI2/SNF2 protein that recycles RNA polymerase during transcription. Structure. 2008; 16:1417–1427. [PubMed: 18786404]
19. Sukhodolets MV, Garges S, Adhya S. Ribosomal protein S1 promotes transcriptional cycling. RNA. 2006; 12:1505–1513. [PubMed: 16775305]
20. Versteege I, Sevenet N, Lange J, Rousseau-Merck MF, Ambros P, Handgretinger R, Aurias A, Delattre O. Truncating mutations of *hSNF5/INI1* in aggressive pediatric cancer. Nature. 1998; 394:203–206. [PubMed: 9671307]
21. Sevenet N, Lellouch-Tubiana A, Schofield D, Hoang-Xuan K, Gessler M, Birnbaum D, Jeanpierre C, Jouvet A, Delattre O. Spectrum of hSNF5/INI1 somatic mutations in human cancer and genotype-phenotype correlations. Hum. Mol. Genet. 1999; 8:2359–2368. [PubMed: 10556283]
22. Klochendler-Yeivin A, Fiette L, Barra J, Muchardt C, Babinet C, Yaniv M. The murine SNF5/INI1 chromatin remodeling factor is essential for embryonic development and tumor suppression. EMBO Rep. 2000; 1:500–506. [PubMed: 11263494]
23. Guidi CJ, Sands AT, Zambrowicz BP, Turner TK, Demers DA, Webster W, Smith TW, Imbalzano AN, Jones SN. Disruption of *INI1* leads to peri-implantation lethality and tumorigenesis in mice. Mol. Cell. Biol. 2001; 21:3598–3603. [PubMed: 11313485]
24. Roberts CMW, Leroux MM, Fleming MD, Orkin S. Highly penetrant, rapid tumorigenesis through conditional inversion of the tumor suppressor gene. Snf5. Cancer Cell. 2002; 2:415–425.

25. Sukhodolets MV, Garges S. Interaction of *Escherichia coli* RNA polymerase with the ribosomal protein S1 and the Sm-like ATPase Hfq. Biochemistry. 2003; 42:8022–8034. [PubMed: 12834354]
26. Reynolds R, Bermudez-Cruz RM, Chamberlin MJ. Parameters affecting transcription termination by *Escherichia coli* RNA polymerase. I. Analysis of 13 rho-independent terminators. J. Mol. Biol. 1992; 224:31–51. [PubMed: 1372365]
27. Lewis R, Durr H, Hopfner KP, Michaelis J. Conformational changes of a Swi2/Snf2 ATPase during its mechano-chemical cycle. Nucleic Acids Res. 2008; 36:1881–1890. [PubMed: 18267970]
28. Hopfner KP, Michaelis J. Mechanisms of nucleic acid translocases: lessons from structural biology and single-molecule biophysics. Curr. Opin. Struct. Biol. 2007; 17:87–95. [PubMed: 17157498]
29. Haseltine CA, Kowalczykowski SC. An archaeal Rad54 protein remodels DNA and stimulates DNA strand exchange by RadA. Nucleic Acids Res. 2009; 37:2757–2770. [PubMed: 19282450]
30. Roof WD, Young R. jX174 lysis requires *slyD*, a host gene, which is related to the FKBP family of peptidyl-prolyl cis-trans isomerases. FEMS Microbiol. Rev. 1995; 17:213–218. [PubMed: 7669348]
31. Hottenrott S, Schumann T, Pluckthun A, Fischer G, Rahfeld JU. *Escherichia coli* SlyD is a metal ion-regulated peptidyl-prolyl *cis*/*trans*-isomerase. J. Biol. Chem. 1997; 272:15697–15701. [PubMed: 9188461]
32. Scholz C, Eckert B, Hagn F, Schaarschmidt J, Balbach J, Schmid FX. SlyD proteins from different species exhibit high prolyl isomerase and chaperone activities. Biochemistry. 2006; 45:20–33. [PubMed: 16388577]
33. Leach MR, Zhang JW, Zamble DB. The role of complex formation between the *Escherichia coli* hydrogenase accessory factors HypB and SlyD. J. Biol. Chem. 2007; 282:16177–16186. [PubMed: 17426034]
34. Mitterauer T, Nanoff C, Ahorn H, Freissmuth M, Hohenegger M. Metal-dependent nucleotide binding to the *Escherichia coli* rotamase SlyD. Biochem J. 1999; 342:33–39. [PubMed: 10432297]
35. Mukherjee S, Shukla A, Guptasarma P. Single-step purification of a protein-folding catalyst, the SlyD peptidyl prolyl isomerase (PPI), from cytoplasmic extracts of *Escherichia coli*. Biotechnol Appl. Biochem. 2003; 37:183–186. [PubMed: 12630907]
36. Parsy CB, Chapman CJ, Barnes AC, Robertson JF, Murray A. Two-step method to isolate target recombinant protein from co-purified bacterial contaminant SlyD after immobilized metal affinity chromatography. J. Chromatogr. B Analyt Technol. Biomed. Life Sci. 2007; 853:314–319.
37. Bork P, Koonin EV. An expanding family of helicases within the DEAD/H superfamily. Nucleic Acids Res. 1993; 21:751–752. [PubMed: 8382805]
38. Kolsto AB, Bork P, Kvaloy K, Lindback T, Gronstadt A, Kristensen T, Sander C. Prokaryotic members of a new family of putative helicases with similarity to transcription activator SNF2. J. Mol. Biol. 1995; 230:684–688. [PubMed: 8464078]
39. Roberts RW, Crothers DM. Stability and properties of double and triple helices: dramatic effects of RNA or DNA backbone composition. Science. 1992; 258:1463–1466. [PubMed: 1279808]
40. Morvan F, Imbach JL, Rayner B. Comparative stability of eight triple helices formed by differently modified DNA or RNA pyrimidine strands and a DNA hairpin. Antisense Nucleic Acid Drug Dev. 1997; 7:327–334. [PubMed: 9303184]
41. Ivanov S, Alekseev Y, Bertrand JR, Malvy C, Gottikh MB. Formation of stable triplexes between purine RNA and pyrimidine oligodeoxyxylonucleotides. Nucleic Acids Res. 2003; 31:4256–4263. [PubMed: 12853644]
42. Drolet M, Broccoli S, Rallu F, Hraiky C, Fortin C, Masse E, Baaklini I. The problem of hypernegative supercoiling and R-loop formation in transcription. Front. Biosci. 2003; 8:210–221.
43. Komissarova N, Kashlev M. Transcriptional arrest: *Escherichia coli* RNA polymerase translocates backward, leaving the 3’ end of the RNA intact and extruded. Proc. Natl. Acad. Sci. USA. 1997; 94:1755–1760. [PubMed: 9050851]
44. Marr M, Roberts JW. Function of transcription cleavage factors GreA and GreB at a regulatory pause site. Molecular Cell. 2000; 6:1275–1285. [PubMed: 11163202]

45. Nudler E, Mustaev A, Lukhtanov E, Goldfarb A. The RNA-DNA hybrid maintains the register of transcription by preventing backtracking of RNA polymerase. Cell. 1997; 89:33–41. [PubMed: 9094712]

46. Banerjee S, Chalissery J, Bandey I, Sen R. Rho-dependent transcription termination: more questions than answers. J. Microbiol. 2006; 44:11–22. [PubMed: 16554712]

47. Durr H, Korner C, Muller M, Hickman V, Hopfner K-P. X-Ray structure of the *Sulfolobus solfataricus* SWI2/SNF2 ATPase core and its complex with DNA. Cell. 2005; 121:363–373. [PubMed: 15882619]

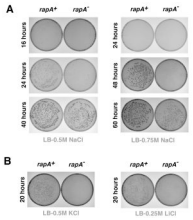

Figure 1. *In vivo* effects of the *rapA* deletion mutation. A
Kinetics of the *E. coli* MG1655*rapA*$^{+}$ and MG1655*rapA*$^{-}$ cells' growth on LB-agar plates containing elevated concentrations of sodium chloride. **B**. Effects of KCl and LiCl on growth of the two strains on LB-agar.

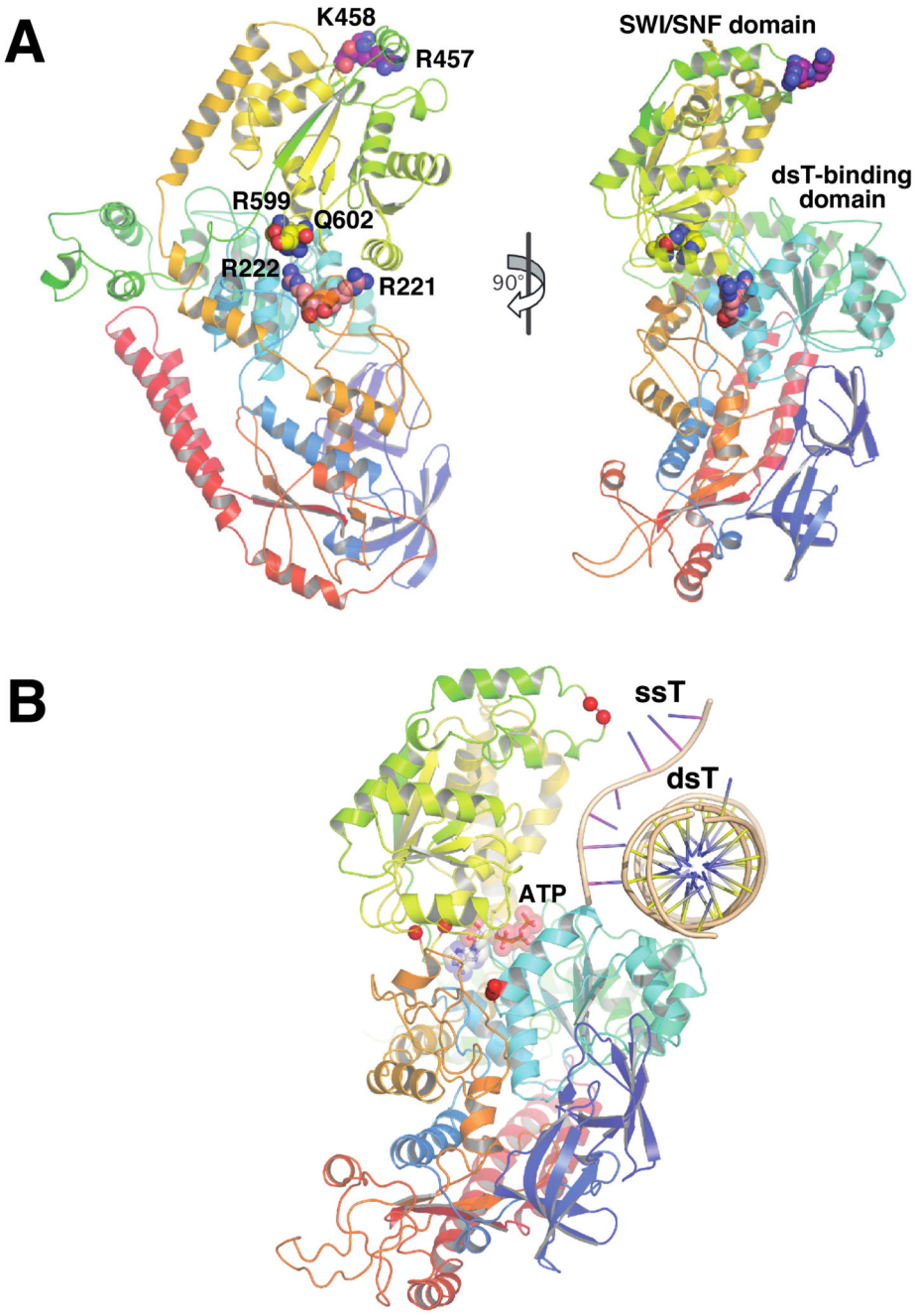

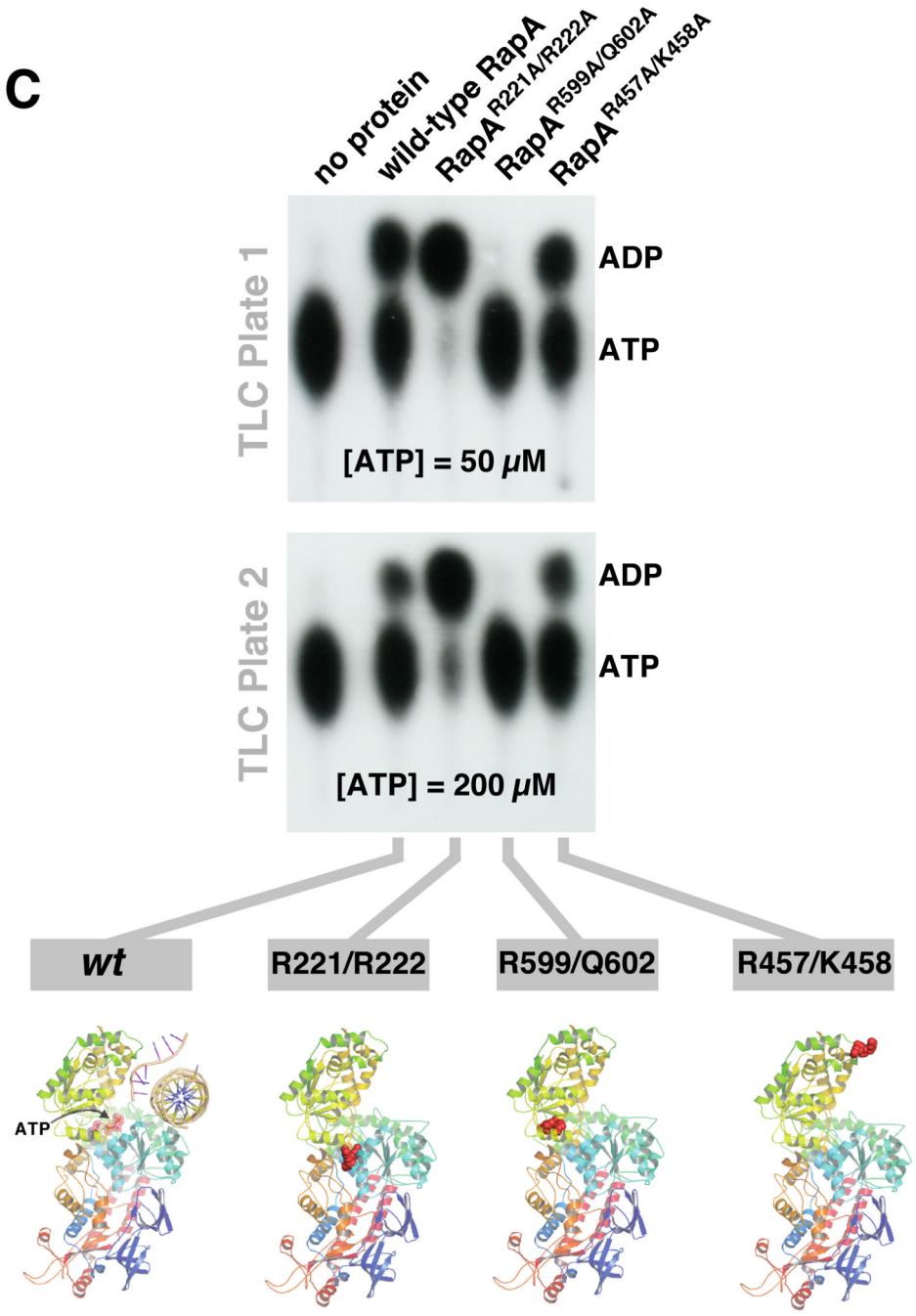

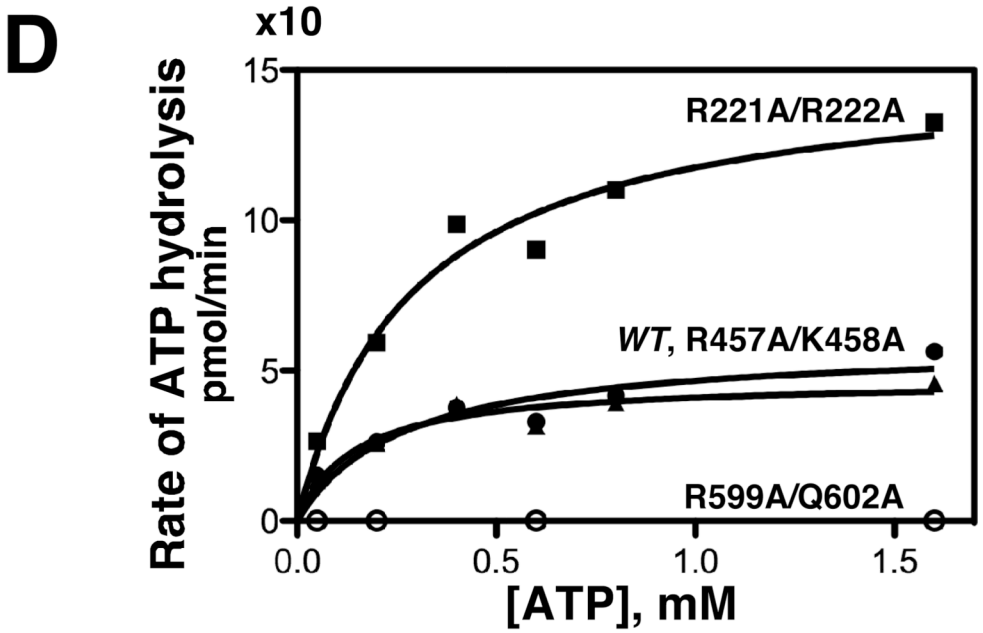

parameter / protein	$K_{m,\ ATP}$ mM	V_{max} pmol/min
wild-type RapA	0.26±0.13	58.9±8.8
$RapA^{R221A/R222A}$	0.29±0.08	151.1±14
$RapA^{R599A/Q602A}$	ND	ND
$RapA^{R457A/K458A}$	0.15±0.06	46.9±4.3

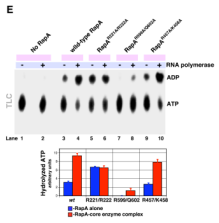

Figure 2. Effect of the mutations in RapA's SWI/SNF domain and its interface with the putative double-stranded nucleic acid-binding domain on the ATP-hydrolytic activity of RapA

A and **B** Positions of the selected mutation sites in the RapA structure. For clarity, only the backbone of the RapA structure (18) is shown; the mutated amino acids are shown as spheres. Figure **2B** also shows the hypothetical positions of a double-stranded nucleic acid template (dsT; a cross-sectional view is shown) and a single-stranded nucleic acid template (ssT). The dsT position (17,18) is determined solely on the basis of modeling using the *Sso*Rad54–DNA complex (47) as a template; no available data conclusively rule out RNA as a dsT. SsT binding by RapA's SWI/SNF domain is also supported by the modeling data (18). The composite model shown in Figure **2B** was constructed as described by Shaw *et al.* (18), essentially by mapping the ATP and nucleic acid-binding sites (both single- and double-stranded DNA) from available crystal structures of the ternary PcrA-ATP-DNA and binary *Sso*Rad54-DNA complexes onto the *E. coli* RapA structure (PDB 3DMQ), followed by manual adjustment and energy minimization. **C** and **D**. Mutations in the interface of RapA's putative dsT-binding and SWI/SNF domains significantly alter its ATP hydrolytic activity. ATPase assays were carried out in Buffer D, as described in Materials and Methods. Representative PEI-cellulose plates illustrating the ATP hydrolysis by the wild-type and recombinant mutant RapA proteins are shown in Figure **2C**. Kinetic parameters (K_m and V_{max}) summarized in Figure **2D** were obtained from the initial velocity of ATP hydrolysis *vs*. the ATP concentration plots (shown at the top) using Prism 5 Software (GraphPad). The parameters were calculated assuming classic Michaelis-Menten kinetics. ND: not detectable. **E**. Effect of the core RNA polymerase on ATP-hydrolytic activity of the wild-type and mutant RapA proteins. ATPase assays were carried out in Buffer D, as described in Materials and Methods. Reactions in the absence (lanes 1, 3, 5, 7, and 9) or in the presence of 2 mol of the purified core RNA polymerase per mol RapA (lanes 2, 4, 6, 8, 10) are shown. Quantitated results of the experiment are shown below; data represent the average of two independent sets of experiments.

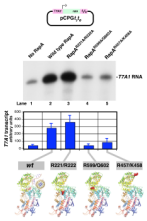

Figure 3. Effect of the mutations in RapA's SWI/SNF domain and its interface with the putative double-stranded nucleic acid-binding domain on RapA's transcription-stimulatory activity

In vitro transcription reactions with the supercoiled DNA template pCPGt_3t_e (26) containing the *T7A1* promoter were carried out in Buffer C for 60 min in the absence (lane 1) or in the presence of 0.36 μM recombinant wild-type (lane 2) or mutant RapA proteins (lanes 3–5) as described in Materials and Methods. Supercoiled DNA template, 0.032 μg/μl; purified RNA polymerase holoenzyme, 0.023 μg/μl. Following the addition of Stop solution, the reactions were denatured by boiling and the ^{32}P-labeled RNA transcripts were fractionated on 8% SequaGel (National Diagnostics). Quantitated results of the experiment are shown at the bottom; data represent the average of two independent sets of experiments.

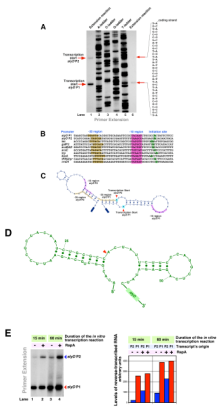

Figure 4. Mapping of the transcription initiation site(s) at the *E. coli slyD* operon. A
Determination of the transcription start site(s) at the *slyD* operon. Primer extension reactions (lanes 1 and 6) resulting from extension of the DNA primer MS702 (see Materials and Methods) by M-MuLV Reverse Transcriptase from the *slyD* mRNA template(s) synthesized *in vitro*. Lanes 2–5 show the DNA sequencing ladder – the result of extension of the same primer by *Taq* DNA polymerase. **B**. Conserved elements (boxes shown in magenta and yellow) and the transcription start sites (green boxes) of the *slyD* P1 and P2 promoters. *SlyD* P1 and *slyD* P2 promoters are aligned against several well-studied *E. coli* promoters. **C**. The *slyD* operon's conserved elements and the transcription start sites are shown on the coding DNA strand folded into the hypothetical lowest-energy secondary structure; the template strand is not shown. **D**. The nontranslated 5'-terminus of the *slyD* mRNA originating at the P2 promoter. The lowest-energy secondary structure is shown. The red arrowhead points to the 5'-terminus of the *slyD* mRNA originating at the P1 promoter. **E**. The effect of RapA on transcription at the *slyD* operon. *In vitro* transcription reactions were carried out as described in Materials and Methods. Medium-duration (15-min) reactions (lanes 1 and 2) and long-duration (60-min) reactions (lanes 3 and 4) were carried out in the presence or absence of excess (1 μM) wild-type RapA. Primer extension analysis of the RNAs synthesized *in vitro* was carried out as described in Materials and Methods. Note that RapA has little or no effect on P1-driven transcription, but has a positive (4–5-fold) stimulatory effect on transcription initiated at P2. The quantitated levels of reverse-transcribed RNAs are shown at the right.

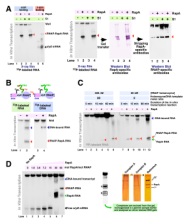

Figure 5. RapA contributes to the formation of free (non-DNA-bound or aggregated) RNA during *in vitro* transcription. I: Fractionation and identification of RapA-specific intermediates under semi-denaturing conditions. A

Formation of RapA-specific complexes in *in vitro* transcription system with linear DNA templates encompassing the *E. coli slyD* operon. *In vitro* transcription reactions in the absence of effectors (lanes 1 and 5), in the presence of 1 μM of purified recombinant RapA (lanes 2 and 6), 1 μM purified recombinant S1 (lane 3), or 1 μM RapA plus 1 μM S1 (lane 4) were carried out as described in Materials and Methods, and the reaction products were separated on 6% SequaGel (National Diagnostics). Reaction conditions: Buffer D (see Materials and Methods); purified 965-nt linear DNA template containing the *slyD* operon (PCR MS696/697), 7 nM; RNA polymerase holoenzyme, 20 nM. Reactions not denatured by boiling are in lanes 1–4; reactions in lanes 5 and 6 are identical to those in lanes 1 and 2 except that the samples were subjected to a 1-min boiling step followed by placement on ice after the addition of Stop solution. RNA polymerase-RapA-transcript complexes are indicated with red arrowheads. *Panels at the right*: identification of the *in vitro* transcription reaction intermediates through a combination of uniform ^{32}P RNA labeling and immunoassays. Following electrophoresis, X-ray films were exposed to 'wet' gels to visualize ^{32}P-labeled RNA transcripts. Next, the contents of the gels were electroeluted onto Hybond-P membranes (Amersham Pharmacia Biotech) for immunoassays, first with RapA-specific and next with RNA polymerase-specific antibodies (sequentially, using the same membrane, after stripping the RapA-specific antibodies). **B**. Identification of DNA-bound complexes formed during *in vitro* transcription with linear DNA templates encompassing the *slyD* operon through selective ^{32}P labeling of RNA or DNA. *In vitro* transcription reactions in the absence of RapA (lane 1) or in the presence of 1 μM of purified recombinant RapA (lane 2) were carried out as described in Materials and Methods. Reactions in lanes 3 and 4 were similar to those in lanes 1 and 2 except that ^{32}P end-labeled DNA template and 'cold' rNTP mix was used; the experimental design is illustrated by the schematics above. The *in vitro* transcription reaction products were separated on 4.5% SequaGel (National Diagnostics). **C**. Kinetics of the formation of free (non-DNA-bound or aggregated) RNA polymerase-transcript complexes in the presence of RapA. *In vitro* transcription reactions were carried out as described in Materials and Methods in the absence of RapA (lanes 1, 3, 5, 7, 9, 11) or in the presence of 1 μM wild type recombinant RapA (lanes 2, 4, 6, 8, 10, 12), and the reaction products were resolved on 5% SequaGel (National Diagnostics). Reaction conditions: Buffer D; purified 965-nt linear DNA template containing the *slyD* operon (PCR MS696/697), 25 nM. The RNA polymerase holoenzyme concentrations are indicated in the figure. RNA polymerase-RapA-transcripts (red arrowhead), RapA-RNA adducts (green arrowhead), and DNA-bound transcripts (blue arrowhead) are also indicated. **D**. Titration with purified RapA of *in vitro* transcription reactions with the *slyD* operon. Reactions were carried out in Buffer D, as described in Materials and Methods, and the reaction products were resolved on 4.5% SequaGel (National Diagnostics). Linear DNA template (PCR 696/697), 40 nM; RNA polymerase holoenzyme, 50 nM. RNA polymerase-transcript (red arrowhead), RapA-RNA adduct (green arrowhead), and DNA-bound transcript (blue arrowhead) are indicated. *Panels at the right:* to confirm the identity of individual complexes, the bands containing ^{32}P-labeled RNA transcript (highlighted by rectangle frames 'A' and 'B') were dissected from the gel and homogenized in ~200 μl of Laemmli

sample buffer in Eppendorf tube-size disposable homogenizers. Following precipitation of the polyacrylamide slurry by centrifugation, the supernatants were analyzed on silver-stained SDS gels. The reference lane contained the 1:1 RNA polymerase holoenzyme-RapA complex. RapA, σ^{70}, and the large RNA polymerase subunits are indicated; a silver-stained 7% SDS-polyacrylamide gel is shown. Yellow arrowheads ('R') indicate RNA, which was also visualized by silver staining.

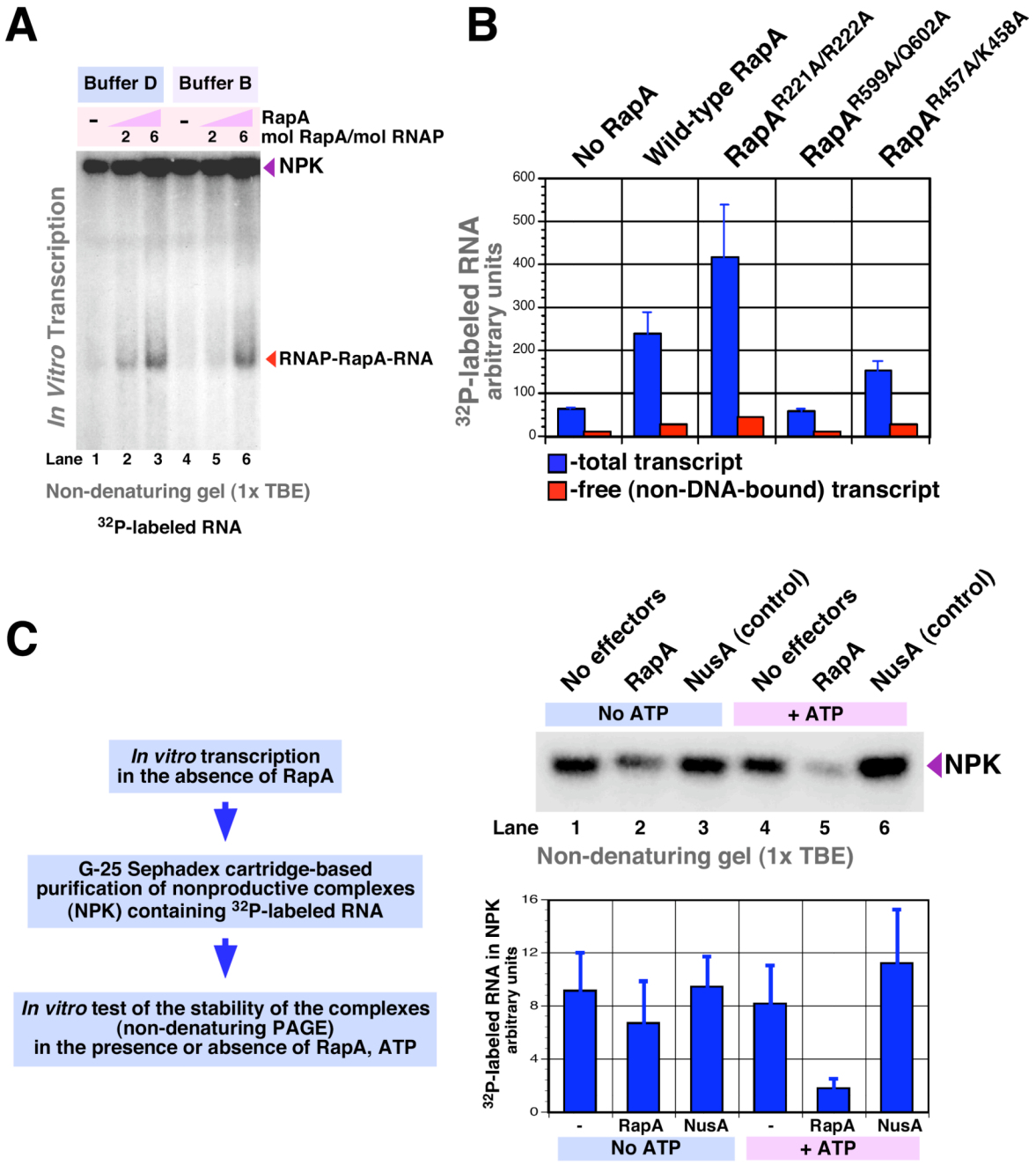

Figure 6. RapA contributes to the formation of free (non-DNA-bound or aggregated) RNA during *in vitro* transcription. II: Fractionation of transcription complexes under non-denaturing conditions. A

RapA promotes the formation of non-DNA-bound or aggregated RNA. *In vitro* transcription reactions were carried out for 30 min at 37°C. Reactions 1–3: Buffer D; reactions 4–6: Buffer B (see Materials and Methods). Other components: purified 965-nt linear DNA template containing the *slyD* operon (PCR MS696/697), 25 nM; RNA polymerase holoenzyme, 50 nM. The RapA/RNA polymerase holoenzyme molar ratios are indicated in the figure. Following the addition of Stop solution, the reaction products were fractionated on 5% ProtoGel (National Diagnostics) containing 1x TBE (KD Medical), using 0.5x TBE

as a running buffer; denaturation of the reactions by boiling was omitted. **B**. Effect of the constructed mutations on RapA's nucleic acid-remodeling activity. *In vitro* transcription reactions similar to those described in Figure 6A were carried out in the presence or absence of 8 mol of wild type or mutant RapA per mol RNA polymerase holoenzyme (50 nM). Reaction products were fractionated by non-denaturing PAGE on 8% ProtoGel, as described in Figure 6A. Graph shows the quantitated levels of total ^{32}P-labeled RNA (blue columns) and non-DNA bound or aggregated RNA (red columns). Data represent the average of two independent sets of experiments. **C**. Effect of RapA on stability of purified nonproductive transcription complexes in the presence or absence of ATP. An *in vitro* transcription reaction similar to that described in Figure 6A, lane 1, was carried out (in the absence of RapA). Following a 30-min incubation, the reaction was diluted to 40 μl with ultrapure water (KD medical) and applied onto a MicroSpin™ G-25 column (Amersham Pharmacia Biotech) pre-equilibrated with ultrapure water. Following centrifugation for 2 min at 700 × g, approximately 40 μl of flow-through was recovered (typically containing 3000–8000 cpm ^{32}P). To test the stability of the purified complexes, 10-μl reactions containing 1x Buffer C, 500–800 cpm transcription complexes purified as described above, 1 mM ATP (if present), and 0.2 μM purified RapA (if present) or NusA (if present, as a control) were incubated for 30 min at 37°C. Next, 4 μl of Stop solution was added to each reaction, and the amount of ^{32}P-labeled RNA retained in the complexes was determined after the samples were fractionated by PAGE on 5% ProtoGel; electrophoresis was carried out as described in Figure 6A. The quantitated data (bottom panel) represent the average of two independent experiments.

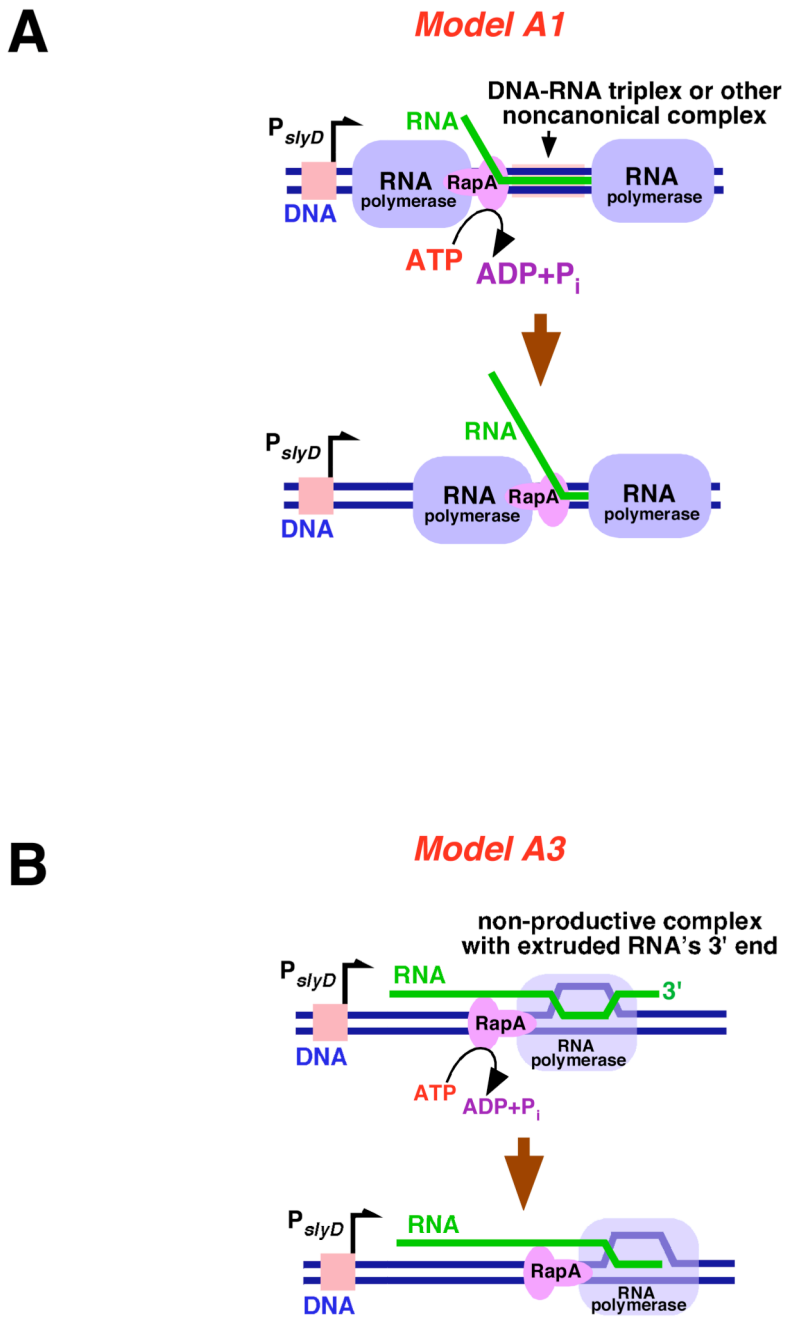

Figure 7. Models explaining possible mechanisms of the RapA-mediated redistribution of RNA during *in vitro* transcription

See text for a detailed discussion of the proposed models. **A**. *Model A1*: RapA lifts RNA transcript from DNA's major groove and/or unwraps RNA from DNA in a processive manner. **B**. *Model A3*: RapA dissociates nonproductive ternary (DNA-RNA polymerase-RNA) complexes with the extruded 3'-end of RNA by either extracting the misaligned RNA or transporting the polymerase along DNA; both activities could contribute to redistribution of RNA in the system and re-initiation of transcription.